Архив патологии
2026, т. 88, №5, с. 29–36
https://doi.org/10.17116/patol20268805129

Russian Journal of Archive of Patology
2026, vol. 88, no. 5, pp. 29–36
https://doi.org/10.17116/patol20268805129

Отличие рецидива от устойчивой ремиссии при остром миелоидном лейкозе. Распределение по стадиям созревания в основных клеточных линиях

© Сергей Эдуардович Есипов[1], Юрий Александрович Криволапов[2]

[1]Quant Isle Ltd, Скарсдейл, Нью-Йорк, США;
[2]ФГБОУ ВО «Северо-западный государственный медицинский университет им И.И. Мечникова» Минздрава России, Санкт-Петербург, Россия

РЕЗЮМЕ

Представлена методология анализа клеток костного мозга при минимальной остаточной болезни (МОБ) в ремиссии острого миелолейкоза (ОМЛ) на основе распределения по стадиям созревания в основных клеточных линиях. Используя атлас BoneMarrowMap (263 159 эталонных клеток, 24 типа клеток) в качестве системы координат, сравнивали каждую клетку в образце костного мозга пациента с МОБ с ее наиболее вероятным нормальным аналогом и относили ее к стадии дифференцировки одной из пяти гемопоэтических линий (миелоидной, эритроидной, В-клеточной, Т-клеточной/естественные киллеры, дендритной). Затем состав костного мозга каждого пациента с МОБ представляли набором гистограмм по стадиям дифференцировки клеточных линий в сравнении с четырьмя эталонными популяциями (здоровый контроль, ОМЛ в момент первичной диагностики, МОБ из которой разовьется рецидив ОМЛ, МОБ в устойчивой ремиссии ОМЛ) посредством расстояний, нормированных на неопределенность классификатора, и коэффициента согласованности соседних стадий τ_{NN}. Применив этот подход к 47 пациентам с ремиссией ОМЛ из четырех независимых когорт (Ennis и соавт., 2023; Lambo и соавт., 2023; Naldini и соавт., 2023; Beneyto-Calabuig и соавт., 2023; данные получены через сводный ресурс Zeng и соавт., 2025), 28 из которых впоследствии рецидивировали, а 19 оставались в устойчивой ремиссии, получили комбинированный набор отличительных признаков, который позволяет достичь площадь под кривой ROC (AUC) 0,95 при перекрестной валидации методом исключения одного объекта, 0,93 при методе исключения двух объектов и 0,92 при повторных стратифицированных разбиениях 70/30. Доминирующим биологическим сигналом была степень зрелости клеточных линий: пациенты, у которых развился рецидив ОМЛ, имели в период ремиссии более высокую долю терминально дифференцированных клеток во всех линиях, особенно плазмоцитоидных дендритных клеток и моноцитов, по сравнению с пациентами, у которых ремиссия ОМЛ устойчиво сохранялась. У пациентов с устойчивой ремиссией обнаруживается в миелоидной ткани более высокая доля примитивных клеток, и ее состав по стадиям дифференцировки клеточных линий больше соответствует костному мозгу здоровых лиц. Эти профили созревания клеточных линий можно получить, используя стандартное одноклеточное РНК секвенирование и общедоступные базы данных.

Ключевые слова: *острый миелолейкоз, минимальная остаточная болезнь, устойчивая ремиссия, прогноз рецидива, секвенирование РНК одиночных клеток, референс-атлас, дифференцировка клеточных линий, распределение по стадиям дифференцировки, согласованность дифференцировки клеточных линий.*

ИНФОРМАЦИЯ ОБ АВТОРАХ:
Есипов С.Э. — https://orcid.org/0000-0003-3006-2037
Криволапов Ю.А. — https://orcid.org/0000-0002-9872-0326
Автор, ответственный за переписку: Криволапов Ю.А. — e-mail: krivolapov.yuri@gmail.com

КАК ЦИТИРОВАТЬ:
Есипов С.Э., Криволапов Ю.А. Отличие рецидива от устойчивой ремиссии при остром миелоидном лейкозе. Распределение по стадиям созревания в основных клеточных линиях. *Архив патологии.* 2026;88(5):29–36.
https://doi.org/10.17116/patol20268805129

Distinguishing relapse from sustained remission in acute myeloid leukemia. Lineage-specific developmental stage distributions

© S.E. Esipov[1], Yu.A. Krivolapov[2]

[1]Quant Isle Ltd, Scarsdale, New York, USA;
[2]I.I. Mechnikov North-Western State Medical University, St. Petersburg, Russia

ABSTRACT

We characterize bone marrow cell populations at minimal residual disease (MRD) by their distribution across hematopoietic developmental stages within each major lineage. Using the BoneMarrowMap atlas (263,159 reference cells, 24 broad cell types) as a coordinate system, we assign each cell in a patient's MRD sample to a developmental stage along one of five lineages (myeloid, erythroid, B-cell, T/natural killer, dendritic). Each patient is then represented by stage histograms compared to four reference populations (healthy control, diagnosis, relapsed MRD, sustained-remission MRD) via uncertainty-normalized distances and adjacent-stage concordance τ_{NN}. Applied to 47 patients from four independent cohorts (Ennis et al. 2023, Lambo et al. 2023,

Naldini et al. 2023, Beneyto-Calabuig et al. 2023; accessed through the Zeng et al. 2025 compendium), 28 of whom relapsed and 19 of whom remained in sustained remission, the combined feature set achieves area under the receiver operating characteristic curve (AUC) 0.95 by leave-one-out cross-validation, 0.93 by leave-two-out, and 0.92 by repeated 70/30 stratified splits. The dominant signal is developmental maturity at MRD: relapsing patients show a higher fraction of terminally differentiated cells across all lineages—particularly plasmacytoid dendritic cells and monocytes—while sustained-remission MRD retains more primitive cells and resembles healthy marrow. These signatures are measurable from standard single-cell RNA sequencing and a public reference atlas.[1]

Keywords: *Acute myeloid leukemia, minimal residual disease, sustained remission, relapse prediction, single-cell RNA sequencing, reference atlas, cell lineage differentiation, developmental stage distribution, adjacent-stage concordance.*

INFORMATION ABOUT THE AUTHORS:
Esipov S.E. — https://orcid.org/0000-0003-3006-2037
Krivolapov Yu.A. — https://orcid.org/0000-0002-9872-0326
Corresponding author: Krivolapov Yu. A. — e-mail: krivolapov.yuri@gmail.com

TO CITE THIS ARTICLE:
Esipov SE, Krivolapov YuA. Distinguishing relapse from sustained remission in acute myeloid leukemia. Lineage-specific developmental stage distributions. *Russian Journal of Archive of Pathology*. 2026;88(5):29–36. (In Engl.). https://doi.org/10.17116/patol20268805129

Introduction

Minimal residual disease (MRD) in acute myeloid leukemia (AML) is the bone marrow state after initial chemotherapy, comprising residual leukemic cells and regenerating normal hematopoiesis. Its composition carries prognostic information, but extracting it requires a reference frame mapping individual cells onto the hematopoietic hierarchy.

Single-cell transcriptomic atlases provide such a reference. BoneMarrowMap, built on the cellular hierarchy framework of Zeng et al. (2022), comprises 263,159 annotated bone marrow cells spanning 55 fine and 24 broad cell types from 45 healthy donors. A softmax classifier over a 54-dimensional shrinkage-LDA space assigns each query cell a predicted type and confidence $\max_i p_i$. The atlas types follow known trajectories: hematopoietic stem cell /multipotent progenitor → lymphoid-primed multipotent progenitor → granulocyte-monocyte progenitor → Monocyte (myeloid); hematopoietic stem cell /multipotent progenitor → megakaryocyte-erythroid progenitor → Erythroblast (erythroid); hematopoietic stem cell /multipotent progenitor → Pro-B → Pre-B → B cell (lymphoid); and so on.

We ask a patient-level question: does the MRD stage distribution, measured along each lineage, differ between patients who will relapse and those who will not? We construct a stage histogram for each patient-lineage pair and compare it to reference histograms from four populations: healthy controls, diagnosis-stage AML, relapsed MRD, and sustained-remission MRD.

Two complementary distances capture histogram similarity: an uncertainty-normalized L_1 distance weighting each stage bin by classifier confidence, and an adjacent-stage concordance τ_{NN} measuring whether local gradients between consecutive stages agree with the reference. Four references×five lineages×two distances yield a 40-dimensional feature vector per patient that robustly discriminates relapse from sustained remission across cross-validation protocols. In Part II of this work, we develop a complementary toolset of ML models that enhances LDA partitions of the BoneMarrowMap and connects to classification. Part II is more technical and is expected to surpass the distribution-based approach of Part I when significantly more data becomes available.

Methods

Reference atlas and classifier

BoneMarrowMap: 263,159 bone marrow cells from 45 healthy donors, 55 fine/24 broad types. A classifier trained by SGD in a 54-dimensional shrinkage-LDA space (Ledoit—Wolf regularized, 55 classes), stage-sequence agnostic, achieved 95% held-out accuracy.

Developmental lineages and stage assignment

The 24 broad cell types were organized into five hematopoietic lineages based on established developmental relationships (**Fig. 1**).

Each query cell was assigned to a lineage based on its predicted broad type. Cells whose predicted type appears in multiple lineages (e.g., hematopoietic stem cell /multipotent progenitor is shared across all five) contribute to each (see **Fig. 1**). The stage histogram for a patient-lineage pair is the vector of fractions: h_k=(number of cells at stage k)/(total cells in that lineage), for k=1, ..., K.

Reference populations

Four reference histograms were computed for each lineage by averaging the stage histograms across patients in each group:

Control: 38 healthy donor samples from 8 cohorts (Bailur, Lasry, Petti, Rodríguez-Meira, van Galen, Zeng, Gawad, Beneyto-Calabuig).

Diagnosis: 272 AML patient samples at initial diagnosis from 21 cohorts.

Relapsed MRD: MRD-phase samples from patients who subsequently relapsed.

Sustained MRD: MRD-phase samples from patients with no recorded relapse.

In cross-validation, relapsed and sustained references were recomputed per fold (training set only); control and diagnosis references were held fixed.

[1]This work was carried out through intensive collaborative sessions with the AI co-author (Claude Opus 4.6, Anthropic), whose ability to write, debug, and iterate analysis code in real time made the scope of this study feasible for a human researcher.

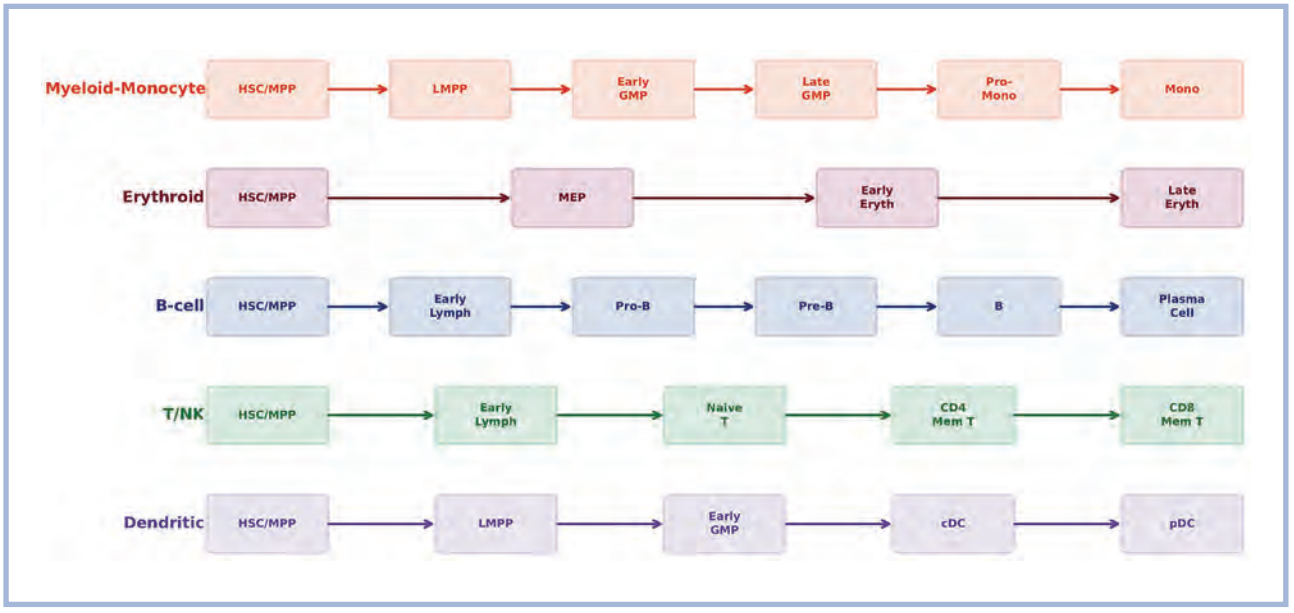


***Fig. 1.* Five hematopoietic lineage chains defined by the BoneMarrowMap atlas.**

Each chain follows the established developmental ordering from HSC/MPP to a terminally differentiated cell type. HSC — hematopoietic stem cell, MPP — multipotent progenitor, LMPP — lymphoid-primed multipotent progenitor, GMP — granulocyte-monocyte progenitor, MEP— megakaryocyte-erythroid progenitor, cDC — conventional dendritic cell, pDC — plasmacytoid dendritic cells.

***Рис. 1.* Пять цепочек кроветворных линий, определенных в атласе BoneMarrowMap.**

Каждая цепочка соответствует установленному порядку развития от гемопоэтических стволовых клеток/мультипотентных предшественников (HSC/MPP) до конечного дифференцированного типа клеток. HSC — гемопоэтическая стволовая клетка, MPP — мультипотентный предшественник, LMPP — лимфоидный праймированный мультипотентный предшественник, GMP — гранулоцитарно-моноцитарный предшественник, MEP— мегакариоцитарно-эритроидный предшественник, cDC —конвенциональные, или классические, дендритные клетки, pDC — plasmacytoid dendritic cells, плазмоцитоидные дендритные клетки.

Distance measures

For each patient at MRD, with stage histogram $h=(h_1, ..., h_k)$ and per-stage classifier confidence $c=(c_1, ..., c_k)$, where c_k is the mean confidence of cells assigned to stage k:

Uncertainty-normalized L_1 distance

$$d_u(h, H)=\sum_{k=1}^{K}\frac{|h_k-H_r|}{1-c_k+c},$$

where H is a reference and ϵ=0.05. Differences in high-confidence stages are amplified; low-confidence differences dampened.

Adjacent-stage concordance

$$\tau_{NN}(h, H)=\frac{1}{K-1}\sum_{k=1}^{K}sign(h_k-h_{k+1})\cdot sign(H_k-H_{k+1}).$$

This measures whether the patient and reference agree on the local gradient between consecutive developmental stages—whether each transition increases or decreases the cell fraction. Unlike the full Kendall τ, which compares all $K(K-1)/2$ pairs including biologically distant stages (e.g., HSC/MPP vs. Monocyte), the adjacent-stage concordance focuses on the $K-1$ transitions that correspond to actual developmental steps in the lineage chain. A patient whose local gradients match the relapsed reference ($\tau_{NN}\approx+1$) but disagree with the sustained reference ($\tau_{NN}\approx-1$) is classified as likely to relapse, regardless of how far the absolute fractions differ.

Feature vector

Each patient at MRD is represented by 4×5=20 uncertainty-normalized distances (4 references ×5 lineages) and 4×5=20 adjacent-stage concordance coefficients, for a total of 40 features.

Classifier

Logistic regression with balanced class weights and l_2 regularization (C=0.5) was applied to the 40-dimensional feature vector. All features were standardized (zero mean, unit variance) using training-set statistics at each cross-validation fold.

Datasets

Single-cell RNA sequencing data for 47 AML patients with MRD-phase samples and known relapse status were drawn from four cohorts in the Zeng et al. (2025) compendium:

— Ennis et al. (2023): 7 patients (7 relapsed, 0 sustained)
— Lambo et al. (2023): 24 patients (20 relapsed, 4 sustained)
— Naldini et al. (2023): 12 patients (1 relapsed, 11 sustained)
— Beneyto-Calabuig et al. (2023): 4 patients (0 relapsed, 4 sustained)

Patients were labeled “relapsed” if a relapse-phase sample existed and “sustained” otherwise (right-censored).

Table 1. **Broad developmental stage fractions by clinical phase (mean across patients)**

Таблица 1. **Фракции основных стадий клеточного созревания в зависимости от клинической фазы (средние значения по пациентам)**

Primitive: HSC/MPP and early multipotent progenitors. Progenitor: committed and late progenitors. Terminal: mature and terminally differentiated cells.

Phase	*n*	Primitive	Progenitor	Terminal
Control	38	0.244	0.232	0.523
Diagnosis	272	0.244	0.428	0.328
MRD — sustained	19	0.155	0.208	0.637
MRD — relapsed	28	0.044	0.219	0.737

Table 2. **Mature cell fractions at MRD by outcome and in healthy controls**

Таблица 2. **Фракции зрелых клеток при минимальной остаточной болезни: сравнительный анализ в зависимости от клинического исхода и показатели у контрольной группы здоровых лиц**

Each value is the fraction of cells within the corresponding lineage that are classified as the terminal cell type

Lineage	Terminal type	Control	Relapsed	Sustained
Myeloid	Monocyte	0.259	0.374	0.235
Erythroid	Late Erythroid	0.379	0.505	0.249
B-cell	B + Plasma Cell	0.344	0.270	0.255
T/natural killer	CD4 + CD8 Memory T	0.413	0.527	0.461
Dendritic	cDC + pDC	0.470	0.604	0.325

Cross-validation protocols

Four cross-validation protocols of increasing stringency were applied:

1. **Leave-one-out (LOO)**: Train on $N-1$ patients, predict 1. All N rotations.
2. **Leave-two-out (L2O)**: Train on $N-2$, predict 2. 200 randomly sampled pairs from $\binom{47}{2}=0.081$.
3. **Leave-five-out (L5O)**: Train on $N-5$, predict 5. 200 random draws.
4. **Repeated 70/30 splits**: 200 stratified random splits with 70% train, 30% test.

At each fold, the relapsed and sustained reference histograms were recomputed from the training set. AUC was computed on pooled predictions (L2O, L5O) or averaged across splits (70/30).

Results

Developmental stage distributions differ between clinical phases

Table 1 shows the mean fraction of cells at each developmental depth across clinical phases, aggregated over all lineages. MRD populations are shifted toward terminal differentiation (70% mature) relative to both diagnosis (33%) and healthy controls (52%), with relapsed MRD showing greater terminal enrichment (74%) than sustained MRD (64%). The per-lineage stage distributions are shown in **Fig. 2.**

Per-lineage stage profiles identify discriminative signatures

The dendritic lineage carries the strongest per-lineage signal. At MRD, relapsed patients have significantly higher plasmacytoid dendritic cell fractions (0.281 vs. 0.150, Mann—Whitney $p=0.003$) and conventional dendritic cell fractions (0.323 vs. 0.175, $p=0.003$) than sustained patients. In the myeloid lineage, the Monocyte fraction is elevated in relapse (0.374 vs. 0.235, $p=0.0006$). Table 2 summarizes the mature cell fractions across all lineages.

Relapsed MRD exceeds the healthy control fraction for Monocyte, Late Erythroid, Memory T, and dendritic cells. Sustained MRD falls below the control fraction for all lineages except T/natural killer. The pattern is consistent: relapsed MRD populations are over-mature relative to control; sustained MRD populations are under-mature. Both comparisons are visible in **Fig. 2.**

Table 3. **Effect of distance measure on classification performance (LOO AUC, 47 patients).**

Таблица 3. **Влияние выбора метрики расстояния на операционные характеристики классификации (показатель AUC при перекрестной проверке по методу LOO, 47 пациентов).**

All models use 20 distance features (4 references×5 lineages)

Distance measure	AUC
L_1 unweighted	0.805
L_1 confidence-weighted	0.842
L_1 uncertainty-normalized	0.889

Uncertainty normalization improves classification

Table 3 compares three histogram distance measures on the same 4-reference, 5-lineage feature structure with LOO (Leave-One-Out) evaluation.

Per-stage confidence varies: plasmacytoid dendritic cells have mean confidence 0.90 (relapsed) vs. 0.62 (sustained), while

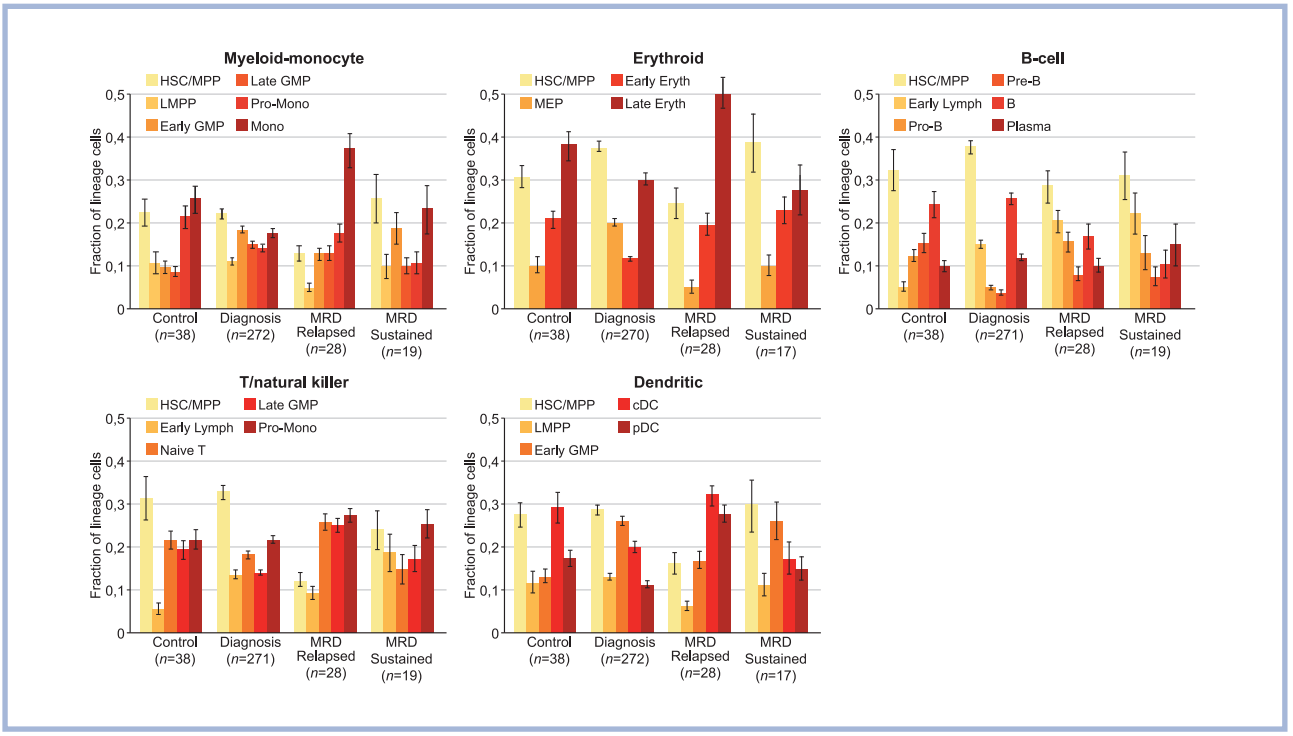


***Fig. 2.* Developmental stage distributions by clinical phase and outcome for each of the five lineages.**

Each panel shows the mean fraction of cells at each developmental stage for four groups: healthy Control, AML Diagnosis, MRD Relapsed, and MRD Sustained. Within each group, bars are arranged from early (light) to late (dark) developmental stages. Error bars show standard error of the mean; *n* indicates the number of patients in each group. Fractions are renormalized per patient before averaging. The progression from diagnosis (early-dominated) through MRD Relapsed (terminal-dominated) is visible in every lineage, while MRD Sustained closely tracks healthy Control.

***Рис. 2.* Распределение стадий развития по клиническим фазам и исходам для каждой из пяти клеточных линий.**

На гистограммах показана средняя доля клеток на каждой стадии развития клеточных линий для четырех групп: «Здоровый контроль», «Диагноз ОМЛ», «МОБ, из которой разовьется рецидив» и «МОБ в устойчивой ремиссии». Внутри каждой группы столбики расположены в порядке от ранних (светлые) к поздним (темные) стадиям развития. Планка погрешности отражает стандартную ошибку среднего значения; *n* обозначает количество пациентов в каждой группе. Доли ренормированы для каждого пациента перед усреднением. Преобладание ранних стадий развития клеток в момент первичной диагностики ОМЛ и терминальных стадий развития клеток при МОБ, из которой разовьется рецидив, наблюдается во всех клеточных линиях. Профиль созревания клеточных линий при МОБ в устойчивой ремиссии практически повторяет профиль созревания у здоровых людей из контрольной группы.

***Table 4.* Classification performance across cross-validation protocols. d_u: uncertainty-normalized distances (20 features).**

***Таблица 4.* Операционные характеристики классификации при различных протоколах перекрестной валидации. d_u: расстояния, нормированные по неопределенности (20 признаков)**

τ_{NN}: within-lineage adjacent-stage concordance (20 features)

Model	Features	LOO	L2O	L5O	70/30
d_u only	20	0.889	0.899	0.876	0.872±0.091
$d_u+\tau_{NN}$	40	0.949	0.926	0.952	0.922±0.073

LMPP sits at ~0.4 in both groups. Inverse-uncertainty weighting amplifies the reliable pDC difference and dampens the noisy LMPP one.

Adjacent-stage concordance adds orthogonal information

Adding within-lineage adjacent-stage concordance τ_{NN} to the uncertainty-normalized distances improves AUC from 0.889 to 0.949, **table 4**. This orthogonal property captures whether the patient's local developmental gradients match the reference, independently of the magnitudes. A patient can have a histogram close to the relapsed reference in absolute terms but with inverted local gradients—the τ_{NN} catches this. Restricting the concordance to adjacent stages (rather than all pairs as in the full Kendall τ) improves performance because the biologically meaningful comparisons are between consecutive developmental stages; comparisons between distant stages (e.g., HSC/MPP vs. Monocyte) are trivially concordant and add noise.

The improvement is consistent across all four protocols, Table 4. The L5O AUC (0.952) exceeds the LOO AUC (0.949), indicating no overfitting: the model generalizes when five patients are held out simultaneously (**Fig. 3**).

Fig. 4 shows the per-patient leave-one-out predictions. Misclassified patients (black outlines) cluster near the decision boundary at *P(relapse)*=0.5.

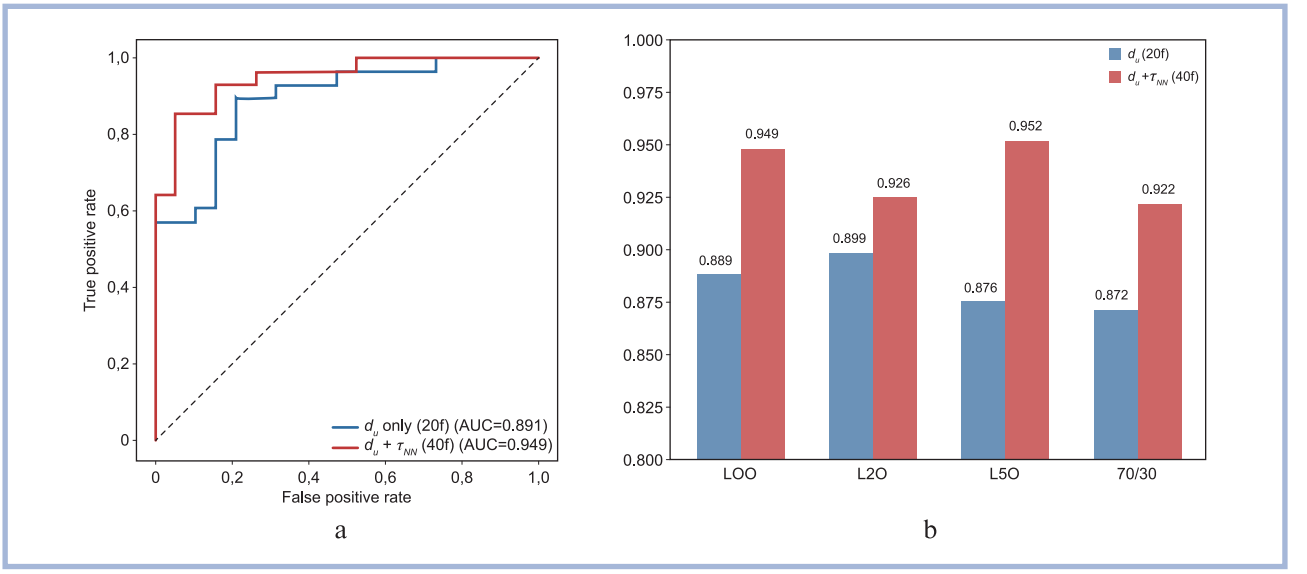


Fig. 3. **Classification performance.**

a — receiver operating characteristic curves for the distance-only model (20 features, blue) and the combined distance + τ_{NN} model (40 features, red), both evaluated by leave-one-out; b — AUC comparison across four cross-validation protocols of increasing stringency.

Рис. 3. **Эффективность классификации.**

a — кривые ROC для модели, основанной только на расстоянии (20 признаков, синий цвет), и комбинированной модели «расстояние + τ_{NN} (40 признаков, красный цвет)», обе модели оценивались методом исключения одного из набора данных; b — сравнение показателя AUC по четырем протоколам перекрестной проверки с возрастающей строгостью.

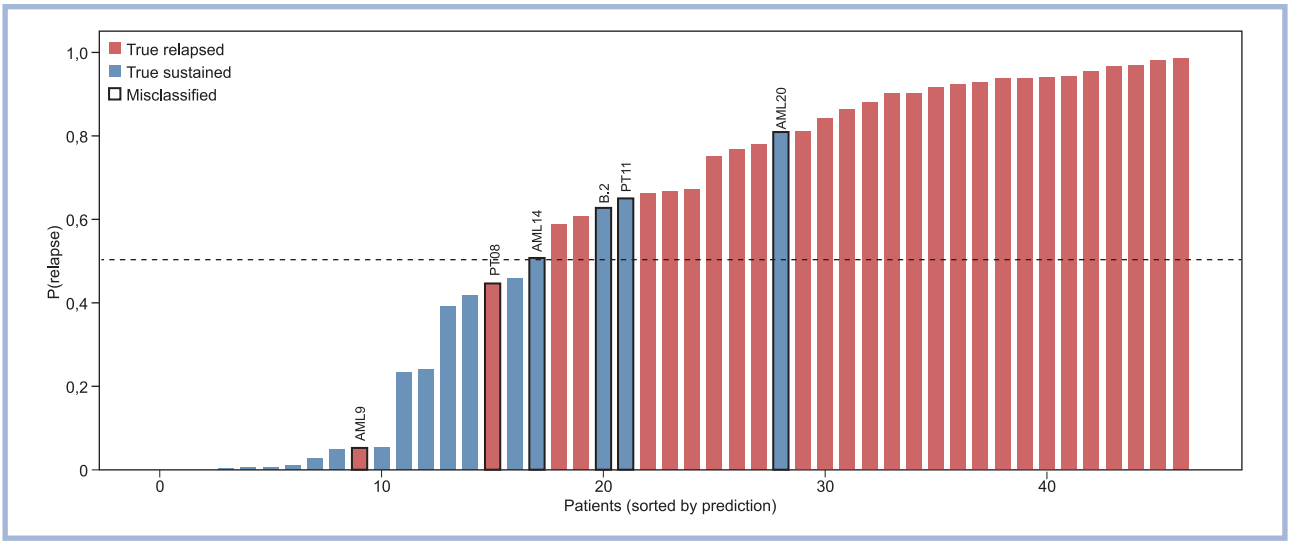


Fig. 4. **Per-patient leave-one-out predictions from the d_u+τ_{NN} model (40 features).**

Each bar represents one patient, colored by true outcome (red: relapsed, blue: sustained). Bars with black outlines indicate misclassifications. Patient identifiers are shown for misclassified cases.

Рис. 4. **Прогнозы методом «один исключен» для каждого пациента, полученные с помощью модели d_u+τ_{NN} (40 признаков).**

Каждый столбик представляет одного пациента; цвет столбика зависит от истинного исхода (красный: рецидив, синий: стабильное состояние). Столбики с черной обводкой обозначают некорректные классификации. Для некорректно классифицированных случаев указаны идентификаторы пациентов.

The developmental ordering is a structural prior, not an empirical optimum

We permuted stage ordering within each lineage (50 random permutations) and recomputed LOO. Since d_u is permutation-invariant, the AUC difference comes entirely from τ_{NN}.

True ordering: AUC 0.949. Random permutations: 0.914±0.033 (range 0.829–0.981); 9/50 exceeded the true ordering. With 47 patients, some lucky orderings overfit, but the atlas ordering is a reliably good prior: it gains +0.060 over distance-only, vs. +0.025 on average for random orderings, and generalizes because it reflects external biology.

Cross-lineage correlations are real but redundant for classification

Per-donor analysis of BoneMarrowMap (45 donors) reveals cross-lineage correlations of mature fractions: myeloid×T/NK p=0.86, myeloid×dendritic p=0.51, myeloid×dendritic p=0.33 (Spearman, p<0.05). These persist at MRD (myeloid×T/NK p=0.82 in relapsed). The lineages share a common HSC/MPP root; their deviations are correlated across patients.

Yet cross-lineage concordance features do not improve classification: pairwise mature-fraction concordance across all 10 pairs (AUC 0.876), top-3 pairs (0.910), full stage×stage across all pairs (0.870), and top-3 pairs (0.949, matching baseline). In every case cross-lineage features degraded or added nothing.

The explanation is redundancy, not independence: each within-lineage feature already captures its share of the common HSC/MPP perturbation. The five lineages are corroborating witnesses to the same event; the classifier gains nothing from knowing they agree.

Discussion

Our central observation: the developmental stage distribution within each lineage—the analog of an age distribution in an interacting population (Esipov, Salueña, 2020) — carries prognostic information at MRD. Just as a forest stand's diameter distribution follows a characteristic geometric decay (de Liocourt, 1898) and shifts predictably under disturbance (Laurance et al., 2004), the stage histogram of a hematopoietic lineage reflects the rates at which cells transition from primitive to mature states. Relapsed patients have distributions skewed toward terminal differentiation; sustained-remission patients retain a more balanced, control-like profile.

The five lineages are correlated (p=0.82 myeloid×T/NK in relapsed MRD), yet cross-lineage features add nothing beyond within-lineage histograms. This signature points to a shared root cause with independent downstream propagation: a perturbation at HSC/MPP sets the initial condition, each chain then runs its own dynamics. The correlation confirms the common origin; the redundancy confirms the absence of inter-lineage coupling. All five lineages shift toward accelerated maturation at MRD in relapsed patients. Under a steady-state assumption, adjacent stage-fraction ratios give transition-rate ratios; at each commitment step (LMPP→Early GMP, MEP→Early Erythroid, HSC/MPP→Early Lymphoid), relapsed patients show 2–4×faster transitions than controls. This lineage-independent acceleration from the shared HSC/MPP compartment is consistent with a cell-intrinsic alteration—most parsimoniously, a pre-leukemic chromatin-regulator mutation (DNMT3A, TET2, ASXL1, IDH1/2) modifying differentiation kinetics without detectable CNV, invisible to inferCNV-based annotation.

Cross-referencing our classifier's predicted cell types with the independent Normal-versus-Malignant annotation in the Lambo et al. (2023) cohort—the only cohort with complete annotation—confirms that the excess mature cells at MRD are overwhelmingly normal, not malignant. In 23 of 24 Lambo patients, Monocytes and plasmacytoid dendritic cells at MRD are 100% Normal by inferCNV. The over-maturation signature therefore reflects aberrant regeneration of normal hematopoiesis, not transcriptional mimicry by residual blasts. A single exception, AML21, shows 99% Malignant monocytes—genuine mimicry—and is notably the patient our classifier struggles with most across all model variants.

Sustained-remission patients tell the complementary story: their MRD distributions are closer to control, suggesting the disease/treatment perturbation heals during recovery. Relapsed distributions diverge from control—a divergence already measurable at MRD, before clinical relapse.

Taken together, these results identify developmental over-maturation across hematopoietic lineages as a quantifiable signature of relapse risk at MRD (leave-one-out AUC 0.95). The signature is measurable from standard single-cell RNA sequencing and a public reference atlas, requiring no trajectory inference, genetic input, or specialized assays.

Limitations

Exploratory analysis

This is pattern discovery on small cohorts, not a validated clinical tool. 47 patients (28 relapsed, 19 sustained) from four cohorts yield AUC estimates with standard deviation ~0.07 across repeated splits. The consistency across cross-validation protocols (LOO 0.949, L2O 0.926, L5O 0.952, 70/30 0.922) and the absence of overfitting (L5O exceeds LOO) are encouraging,; prospective validation on an independent, uniformly processed cohort is required before clinical use.

Right-censoring

Patients labeled as "sustained" had no relapse sample in the compendium, but some may relapse after data collection.

Cohort imbalance

The four cohorts contribute unevenly to the two outcome groups: Ennis et al. (2023) provides 7 relapsed and 0 sustained; Naldini et al. (2023) provides 1 relapsed and 11 sustained. Leave-one-out and leave-two-out cross-validation mix patients across cohorts in every fold, mitigating but not eliminating cohort-specific batch effects.

Atlas dependency

All assignments depend on BoneMarrowMap; systematic atlas biases propagate to the histograms. Within-patient longitudinal comparisons are robust; cross-cohort comparisons may be affected by differing gene overlap with the atlas.

Acknowledgment

We thank Andy G.X. Zeng and John E. Dick for providing access to the AML single-cell compendium that made this study possible. The BoneMarrowMap reference atlas is available at https://github.com/andygxzeng/BoneMarrowMap.

ЛИТЕРАТУРА/REFERENCES

1. Ennis S, Conforte A, O'Reilly E, Takanlu JS, Cichocka T, Dhami SP, Nicholson P, Krebs P, Ó Broin P, Szegezdi E. Cell-cell interactome of the hematopoietic niche and its changes in acute myeloid leukemia. *iScience*.2023;26(6):106943. https://doi.org/10.1016/j.isci.2023.106943
2. Lambo S, Doebele C, Engel C, Beneyto-Calabuig S, Cresswell GD, Strack M, Bitto F, Sill M, Reiss C, Illert AL, et al. A longitudinal single-cell atlas of treatment response in pediatric AML. *Cancer Cell*.2023;41(12):2117-2135.e12. https://doi.org/10.1016/j.ccell.2023.10.008
3. Naldini MM, Casirati G, Barcella M, Ronchi PA, Sarina B, Bresciani A, Vegliante MC, Cuzzola M, Grillo G, Gentner B, et al. Longitudinal single-cell profiling of chemotherapy response in acute myeloid leukemia. *Nat Commun*.2023;14(1):1285. https://doi.org/10.1038/s41467-023-36969-0
4. Beneyto-Calabuig S, Merbach AK, Kniffka J-A, Giber M, Triana S, Acker C, Scharber S, Bechter O, Merz M, Haferlach T, et al. Clonally resolved single-cell multi-omics identifies routes of cellular differentiation in acute myeloid leukemia. *Cell Stem Cell*. 2023;30(5):706-721.e8. https://doi.org/10.1016/j.stem.2023.04.001
5. Zeng AGX, Iacobucci I, Shah S, Mitchell A, Wong G, Bansal S, Chen D, Rathi KS, Yibin L, Kahana S, et al. Single-cell transcriptional atlas of human hematopoiesis reveals genetic and hierarchy-based determinants of aberrant AML differentiation. *Blood Cancer Discov*. 2025;6(4):307-324. https://doi.org/10.1158/2643-3230.BCD-24-0342
6. Zeng AGX, Bansal S, Jin L, Mitchell A, Chen WC, Abbas HA, Chan-Seng-Yue M, Voisin V, van Galen P, Tierens A, et al. A cellular hierarchy framework for understanding heterogeneity and predicting drug response in acute myeloid leukemia. *Nat Med* (2022);28(6):1212-1223. https://doi.org/10.1038/s41591-022-01819-x
7. de Liocourt F. De l'aménagement des sapinières. *Bulletin de la Société forestière de Franche-Comté et Belfort*.1898; 4, 396-409.
8. Esipov S, Salueña C. Synchronization of life cycles by collective transport and emergence of supercycles. *Physical Review.* 2020; E 101, 032412. https://doi.org/10.1103/PhysRevE.101.032412
9. Laurance WF, Oliveira AA, Laurance SG, Condit R, Nascimento HEM, Sanchez-Thorin AC, Lovejoy TE, Andrade A, D'Angelo S, Ribeiro JE, Dick CW. Pervasive alteration of tree communities in undisturbed Amazonian forests. *Nature*. 2004;428:171-175. https://doi.org/10.1038/nature02383

Поступила 12.01.2026
Received 12.01.2026
Принята в печать 24.06.2026
Accepted 24.06.2026